The Sun's atmosphere and magnetic field

- The Sun's corona and magnetic field
- EUV radiation of the corona
- The magnetic network
- Doppler spectroscopy in EUV
- Small-scale dynamics and turbulence
- Temperature profiles in the corona

The visible solar corona

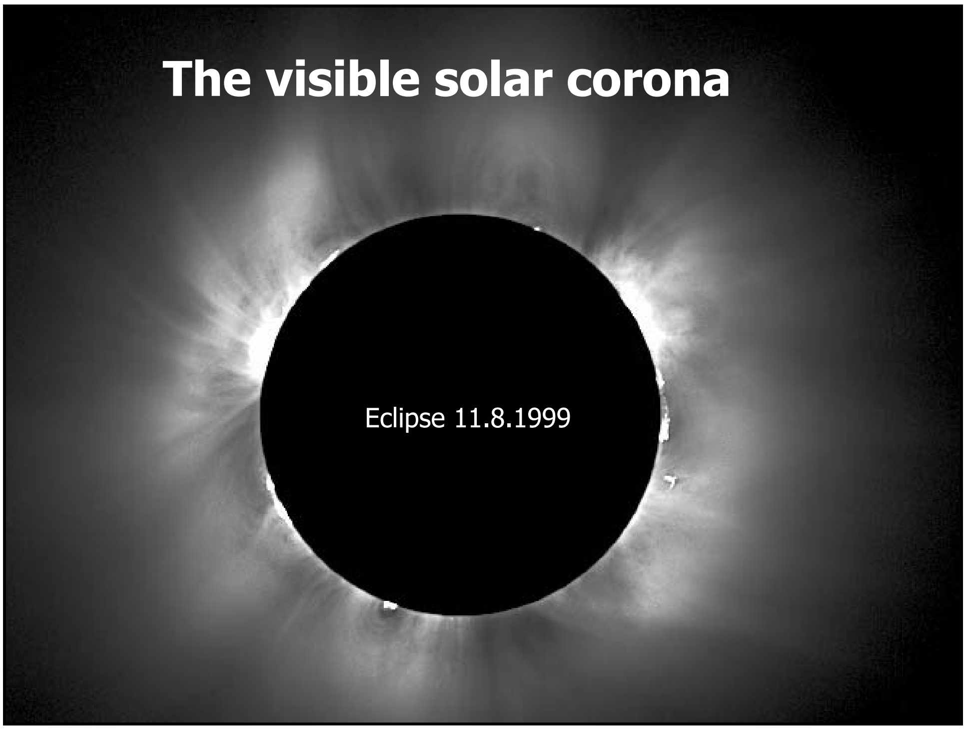

Eclipse 11.8.1999

Electron density in the corona

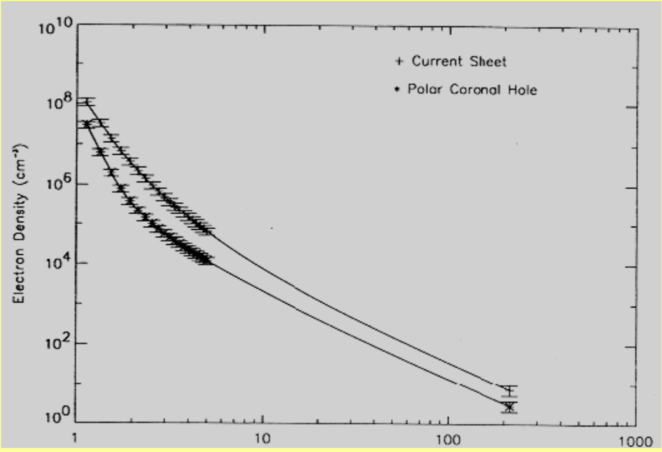

Heliocentric distance / R_s

+ Current sheet and streamer belt, closed

• Polar coronal hole, open magnetically

Guhathakurta and Sittler, 1999, Ap.J., **523**, 812

Skylab coronagraph/Ulysses in-situ

Coronal magnetic field and density

Dipolar, quadrupolar, current sheet contributions

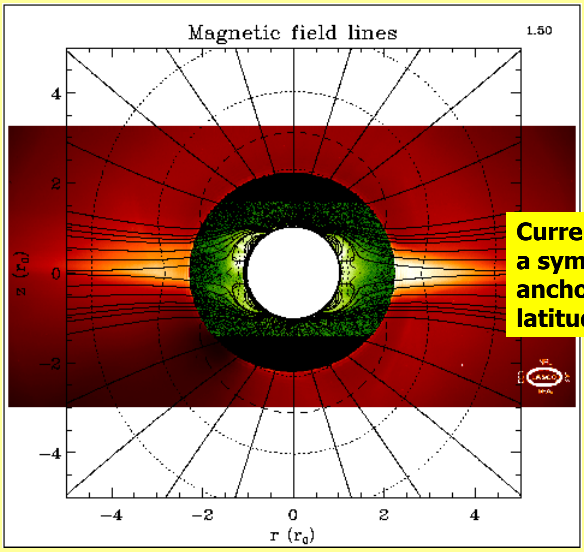

Polar field: B = 12 G

Current sheet is a symmetric disc anchored at high latitudes !

Banaszkiewicz et al., 1998;

Schwenn et al., 1997

LASCO C1/C2 images (SOHO)

Plasma beta I

Starting from the MHD equation of motion for a plasma at rest in a steady quasineutral state, we obtain the simple force balance:

$$\nabla \cdot \mathrm{P} = -\frac{1}{\mu_0}\mathrm{B} \times (\nabla \times \mathrm{B})$$

which expresses ***magnetohydrostatic equilibrium***, in which thermal pressure balances magnetic tension. If the particle pressure is nearly isotropic and the field uniform, this leads to the total pressure being constant:

$$\nabla \left(p + \frac{B^2}{2\mu_0} \right) = 0$$

The ratio of these two terms is called the ***plasma beta***:

$$\beta = \frac{2\mu_0 p}{B^2}$$

Plasma beta II

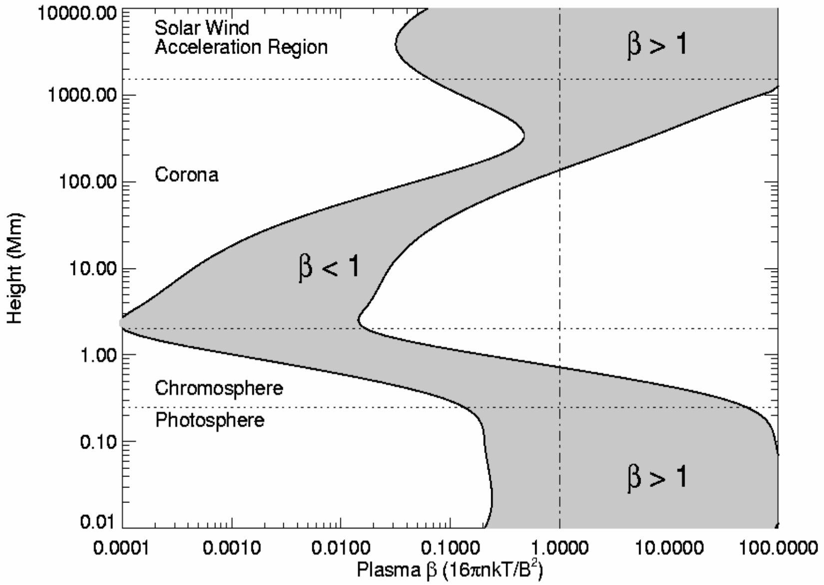

Aschwanden, 2004

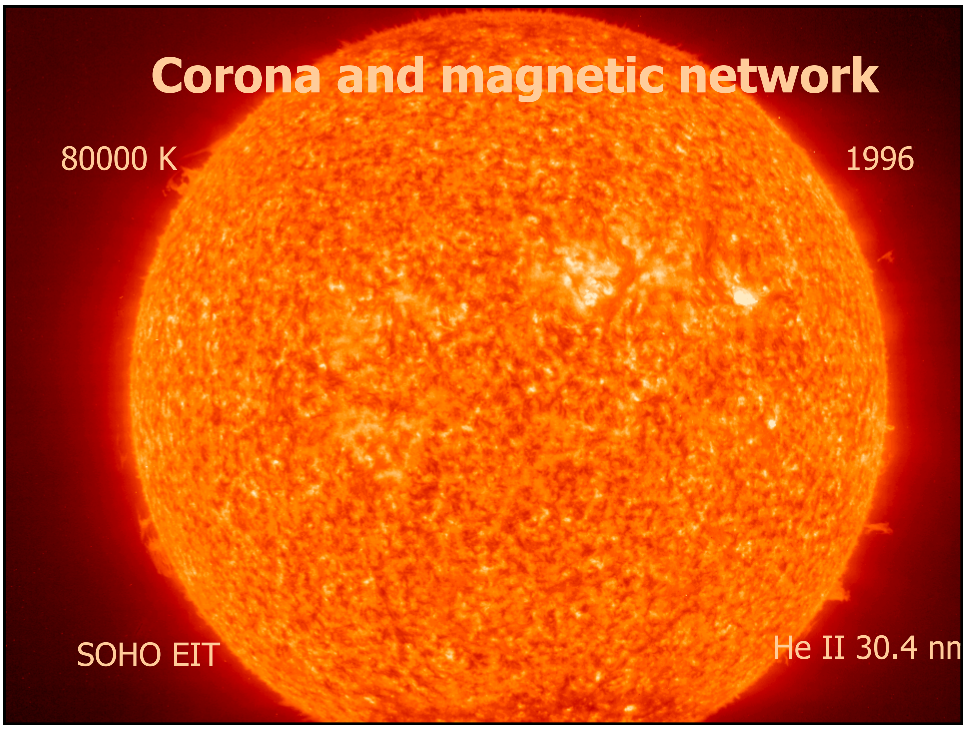

Corona and magnetic network

80000 K

1996

SOHO EIT

He II 30.4 nm

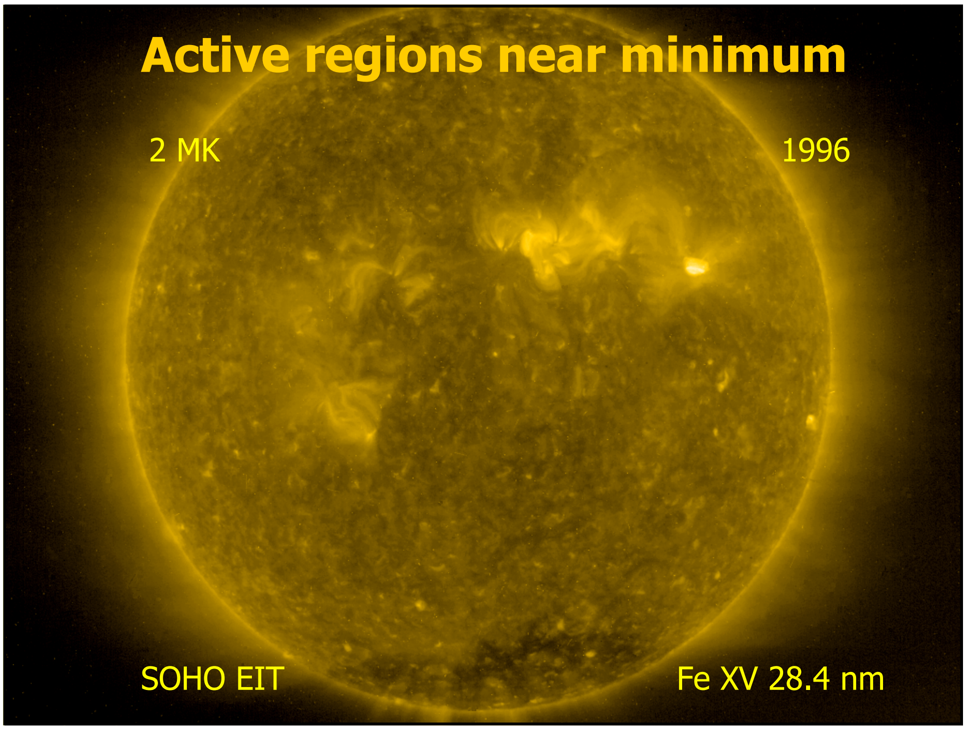

Active regions near minimum

2 MK

1996

SOHO EIT

Fe XV 28.4 nm

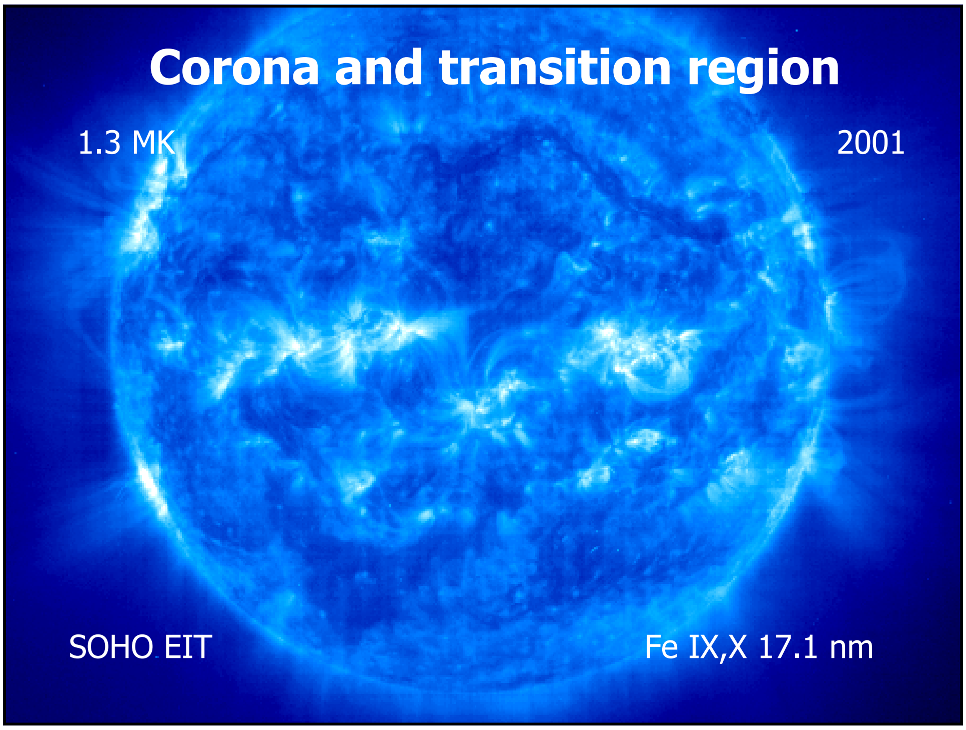

Corona and transition region

1.3 MK

2001

SOHO EIT

Fe IX,X 17.1 nm

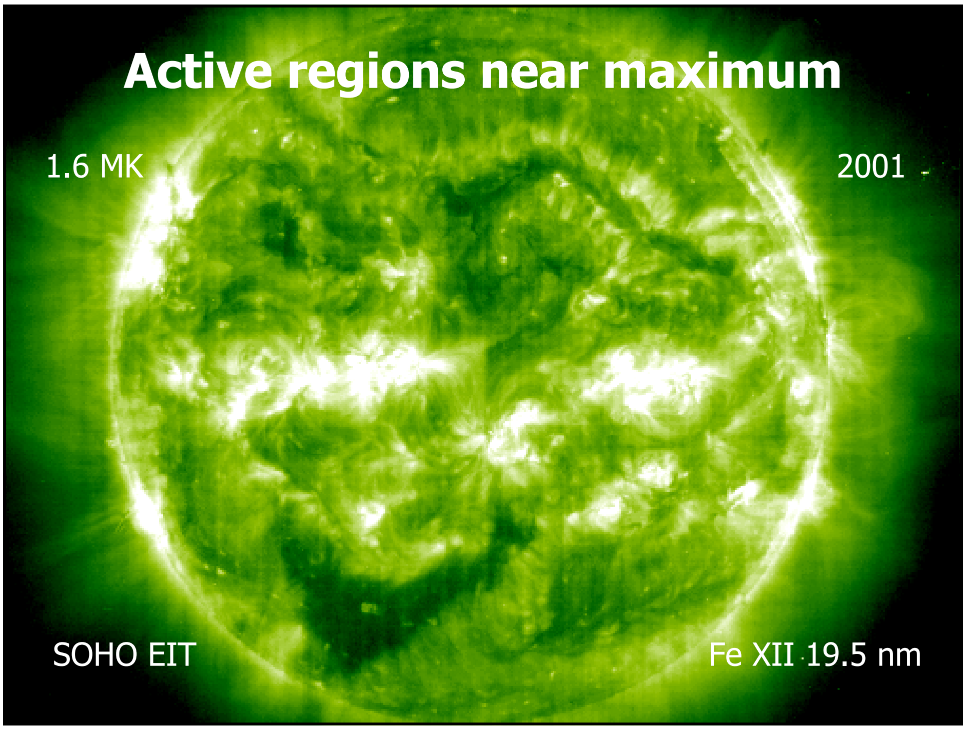

Active regions near maximum

1.6 MK

2001

SOHO EIT

Fe XII 19.5 nm

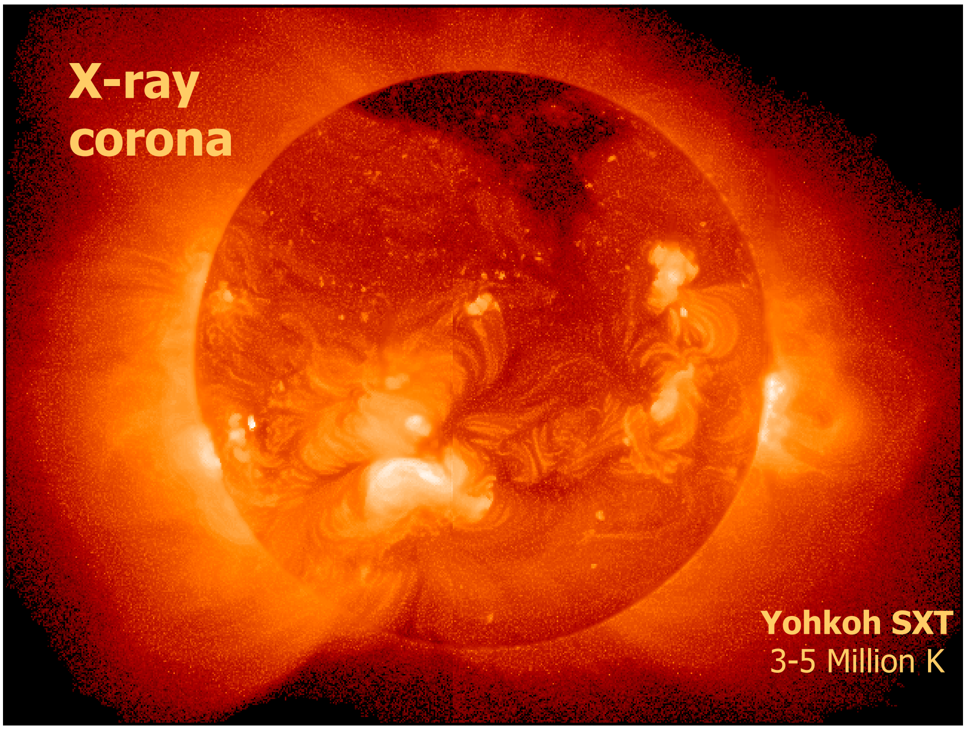

X-ray corona

Yohkoh SXT
3-5 Million K

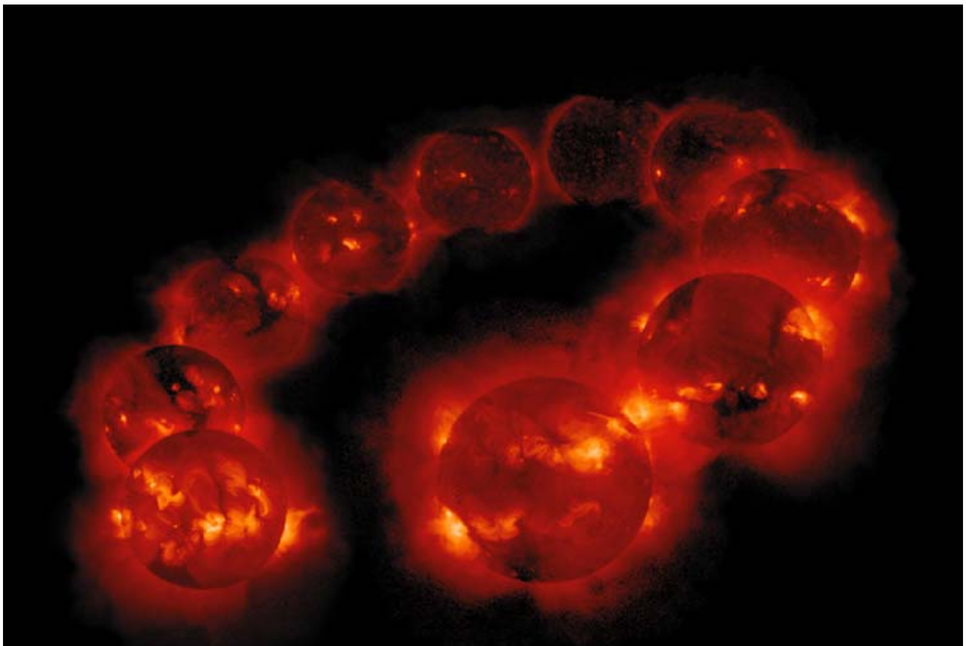

Yohkoh SXT: The changing corona

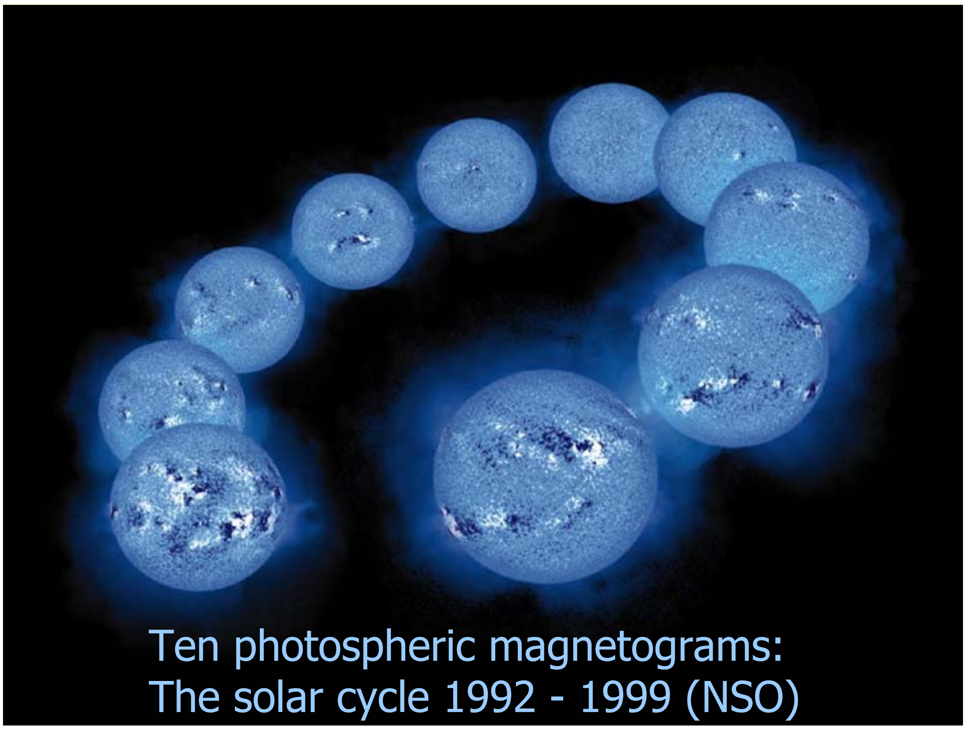

Ten photospheric magnetograms:
The solar cycle 1992 - 1999 (NSO)

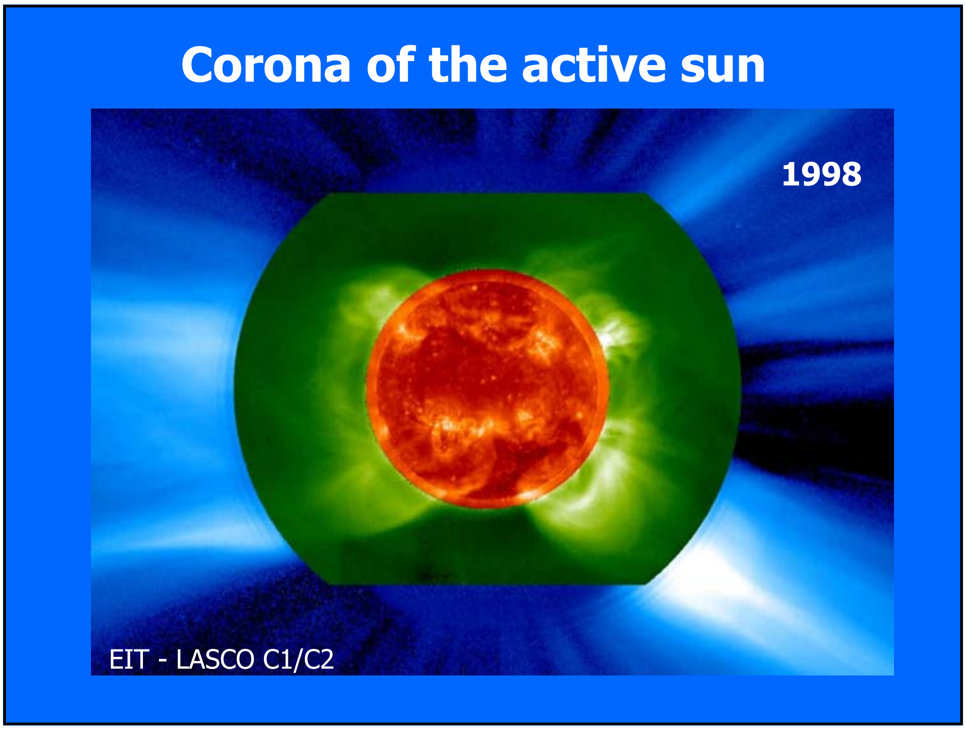

Corona of the active sun

1998

EIT - LASCO C1/C2

North coronal hole in various lines

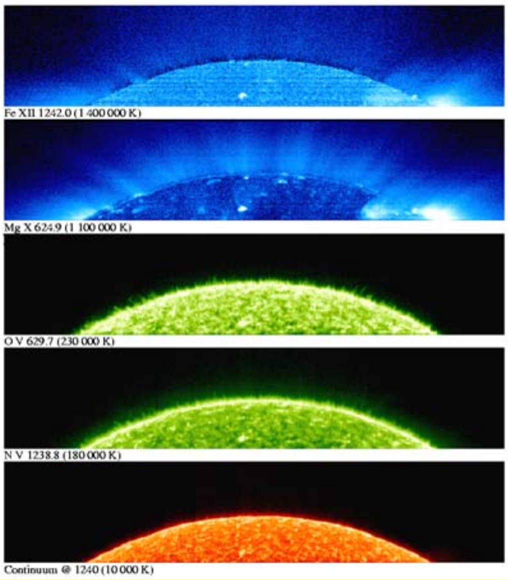

1400000 K	FeXII 1242 Å
1100000 K	MgX 624.9 Å
230000 K	OV 629.7 Å
180000 K	NV 1238.8 Å
10000 K	cont. 1240 Å

Forsyth & Marsch, Space Sci. Rev., **89**, 7, 1999

SUMER/SOHO 10 August 1996

How is the solar corona heated?

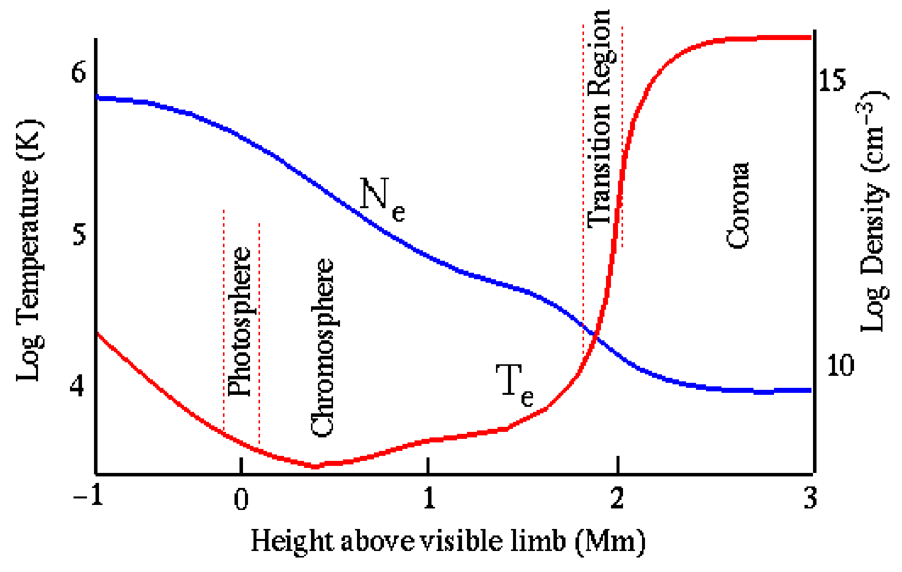

EUV line excitation processes

- *Collisional excitation of atom or ion, A, followed by a radiative decay:*

$A + e^- \rightarrow A^* + e^-$ ($n_e > 10^8\ \mathrm{cm}^{-3}$)

$A^* \rightarrow A + h\nu$ **Line radiance: $L_\lambda \sim n_e^2$**

- *Resonant scattering (fluorescence):*

$A + h\nu \rightarrow A^* \rightarrow A + h\nu$ **Line radiance: $L_\lambda \sim n_e$**

- *Radiative recombination:*

$A^{+z} + e^- \rightarrow A^{+(z-1)*} \rightarrow A^{+z-1} + h\nu$

Solar EUV emission spectrum

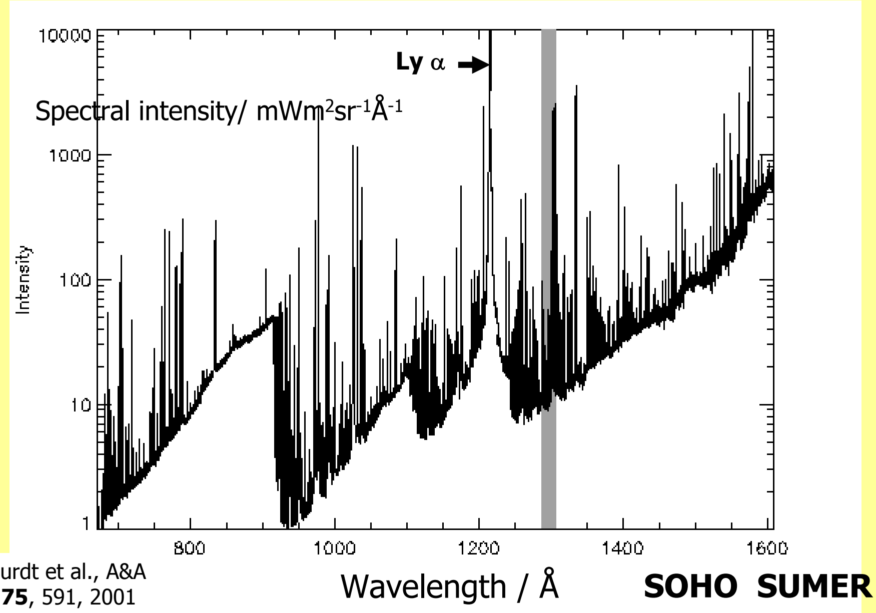

Curdt et al., A&A
375, 591, 2001

SOHO SUMER

Elementary radiation theory I

Coronal model approximation:
collisional excitation and radiative decay

$$N_g(X^{+m})\, n_e\, C_{g,j} \;=\; N_j\, A_{j,g}$$

$C_{g,j}$ [$cm^3 s^{-1}$]	collisional excitation rate
$A_{j,g}$ [s^{-1}]	atomic spontaneous emission coefficient ($\approx 10^{10} s^{-1}$)

Emissivity (power per unit volume):

$$P(\lambda_{g,j}) = N_j(X^{+m})\, A_{j,g}\, \Delta E_{j,g} \qquad [\text{erg cm}^3\, s^{-1}]$$

$\Delta E_{g,j} = E_j - E_g$	photon energy
$N_g(X^{+m})$	number density of ground state of ion X^{+m}

Elementary radiation theory II

Occupation number density of level j of an ion (m-fold ionized atom) of the element X:

$$N_j(X^{+m})/n_e =$$

$$\underset{\substack{\uparrow\\ \text{excitation level}}}{N_j(X^{+m})/N(X^{+m})} \bullet \underset{\substack{\uparrow\\ \text{ionic fraction}}}{N(X^{+m})/N(X)} \bullet \underset{\substack{\uparrow\\ \text{abundance}}}{N(X)/n(H)} \bullet \underset{\substack{\uparrow\\ n(H)\ [cm^3]\ \ \text{hydrogen}}}{n(H)/n_e}$$

Collisonal excitation rate (Maxwellian electrons):

$$C_{i,j} \sim 1/T_e^{1/2} \exp\{ \underset{\substack{\uparrow\\ \text{Boltzmann factor}}}{\Delta E_{i,j}/(k_B T_e)} \}$$

Oxygen ionization balance

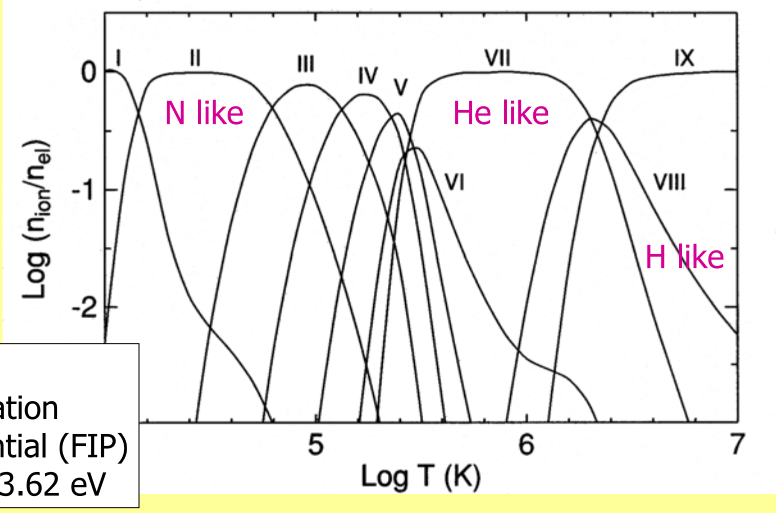

First ionization potential (FIP) I = 13.62 eV

Shull and van Steenberg, ApJ. Suppl. **48**, 95; **49**, 351, 1982

LTE -> $N(X^{+m})/N(X)$ follows from Saha's equation; ~ $\exp(-I/k_BT_e)$

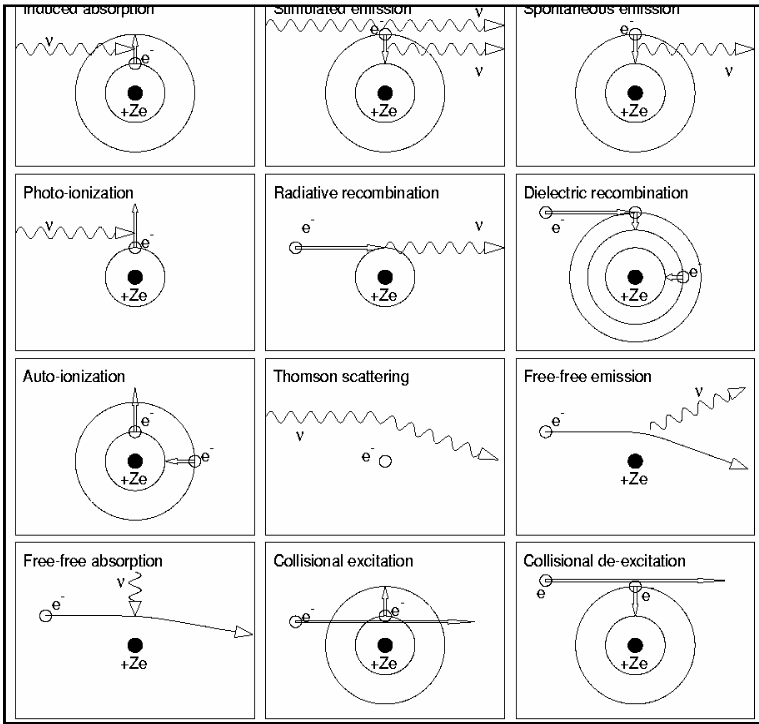

Emission, ionization and recombination processes

Emission measure

Emissivity in the line of ion X^{+m}:

$$P(\lambda_{g,j}) = N(X^{+m})/N(X)\ N(X)/n(H)\ n(H)/n_e\ C_{g,j}\ \Delta E_{g,j}\ n_e^2$$

Contribution function (strongly peaked in T_e):

$$G(T_e, \lambda_{g,j}) = N(X^{+m})/N(X)\ C_{g,j}$$

Emission measure:

$$< EM > \ = \int_V n_e^2\, dV$$

The emission measure depends on the amount of plasma (at temperature T_e) emitting in the observed spectral line.

Radiation power (line strength) ~ < EM >

Loops near the solar limb

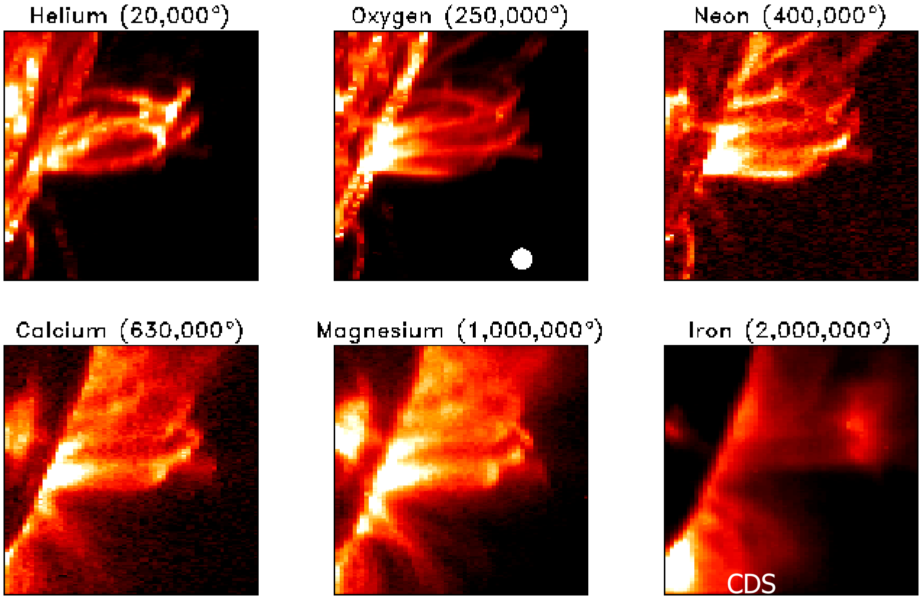

Magnetic loops on the Sun

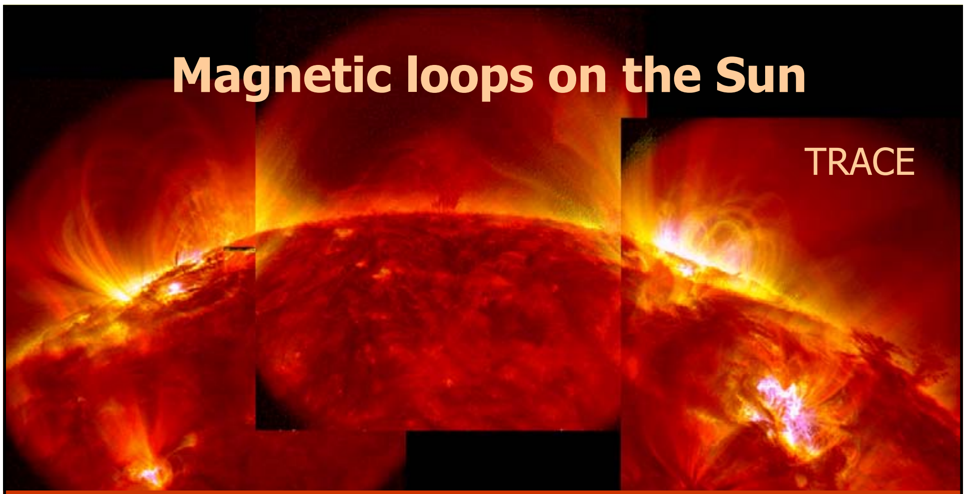
TRACE

- **Thin strands, intrinsically dynamic and continously evolving,**
- **Intermittent heating (in minutes), primarily within 10-20 Mm,**
- **Meandering of hot strings through coronal volume,**
- **Pulsed injection of cool material from chromosphere below,**
- **Variable brightenings, by braiding-induced current dissipation?**

Force-free magnetic field

A special equilibrium of ideal MHD (often used in case of the solar corona) occurs if the beta is low, such that the pressure gradient can be neglected. The stationary plasma becomes ***force free***, if the Lorentz force vanishes:

$$\boxed{\mathbf{j} \times \mathbf{B} = 0}$$

This condition is guaranteed if the current flows along the field and obeys:

$$\boxed{\mu_0 \mathbf{j} = \alpha_L \mathbf{B}}$$

The proportionality factor $\alpha_L(\mathbf{x})$ is called *lapse field*. Ampère's law yields:

$$\boxed{\nabla \times \mathbf{B} = \alpha_L \mathbf{B}}$$

By taking the divergence, one finds that $\alpha_L(x)$ is constant along any field line:

$$\boxed{\mathbf{B} \cdot \nabla \alpha_L = 0}$$

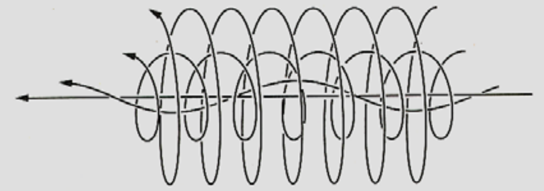

Loop structures

Dipole (potential) field

$\varphi(r, \theta) = - m \cos\theta / r^2 \quad (m = \pi a^2 I / c)$

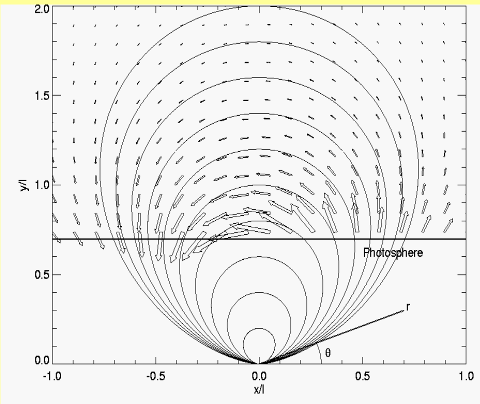

Aschwanden, 2004

$B = \text{grad}\ \varphi$

Sheared (force-free) arcade

$\Delta B + \alpha^2 B = 0 \quad (\tan\theta = \alpha/l)$

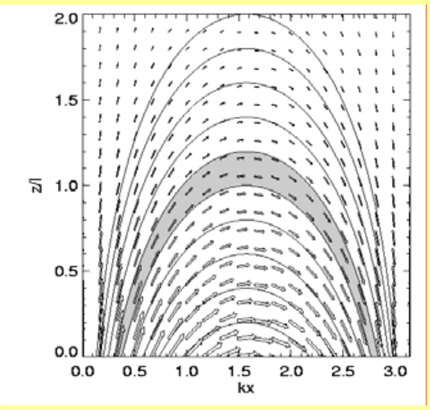

$B_x = B_{x0} \sin(kx) \exp(-lz)$

Evolution of magnetic loops

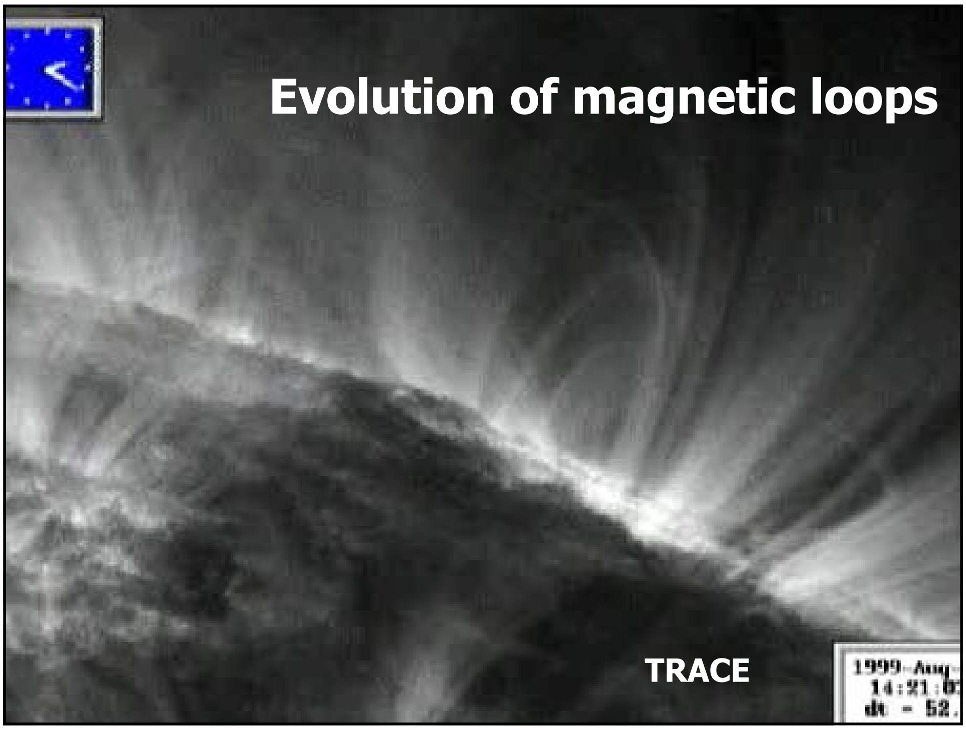

Doppler spectroscopy

- **Line shift** by Doppler effect (bulk motion)

$$v_i = c(\lambda-\lambda_0)/\lambda_0 = c\Delta\lambda_D/\lambda \quad \text{(+, red shift, - blue)}$$

v_i	line of sight velocity of atom or ion;	c	speed of light in vacuo
λ_0	nominal (rest) wave length;	λ	observed wave length

$\varepsilon = h\nu = hc/\lambda = 12345\ \mathrm{eV}/\lambda[\text{Å}]$; 1 eV = 11604 K

- **Line broadening** (thermal and/or turbulent motions)

$$T_{eff} = T_i + m_i\xi^2/(2k_B) = m_i c^2\{(\Delta\lambda_D)^2 - (\Delta\lambda_I)^2\}/(2k_B\lambda^2)$$

$\Delta\lambda_D$ ($\Delta\lambda_I$)	Doppler (instrumental) width of spectral line;	T_i	ion temperature
ξ	amplitude of unresolved waves/turbulence;	m_i	ion mass

For optically thin emission and Gaussian line profile; $\Delta\lambda_I \approx$ 6 pm for SUMER

Cool loop in transition region

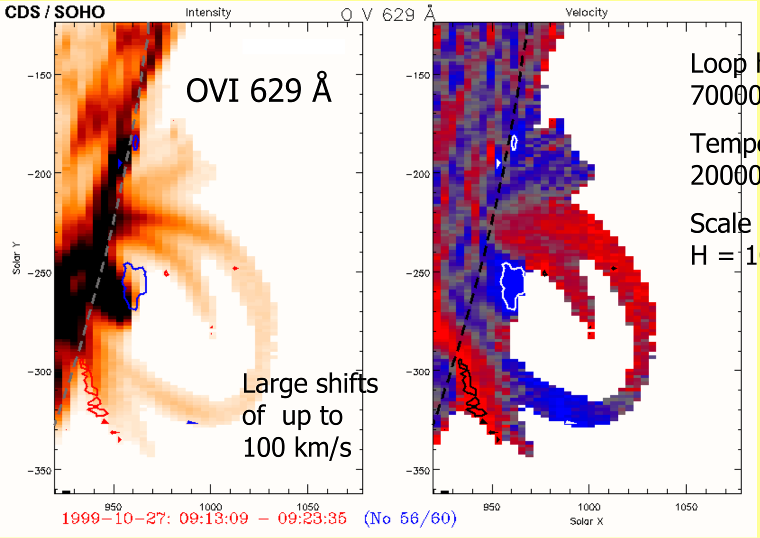

OVI 629 Å

Large shifts of up to 100 km/s

Loop height: 70000 km

Temperature: 200000 K

Scale height: H = 10000 km

CDS/SOHO web page

How can cool material reach this height?

Doppler shift versus temperature

Dopplershifts (SUMER) in the transition region (TR) of the „quiet" sun

- Blueshifts in lower corona (MgX and NeVIII line), outflow
- Redshifts in upper TR, plasma confined

Peter & Judge, ApJ. **522,** 1148, 1999

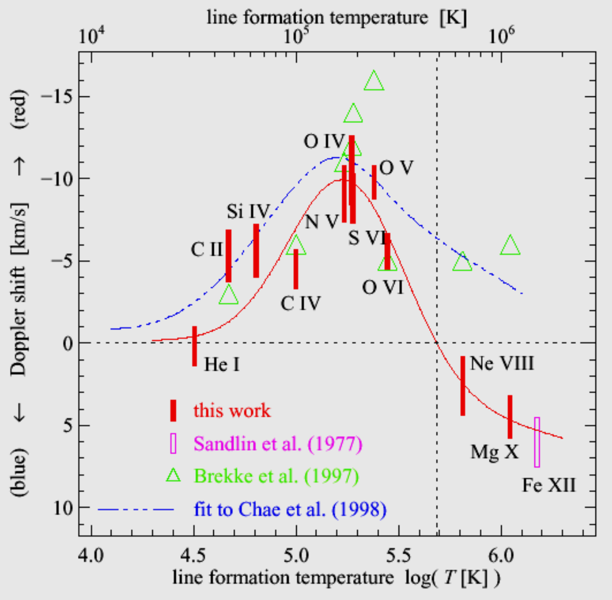

Nonthermal line broadening

Line widths:

I wing

I core

- Width of wing increases and reaches local sound speed!
- $\xi \sim T^{1/4}$, as for undamped Alfvén waves
- F_A = 1 kWm^{-2} B/G

Peter, A&A **374**, 1108, 2001

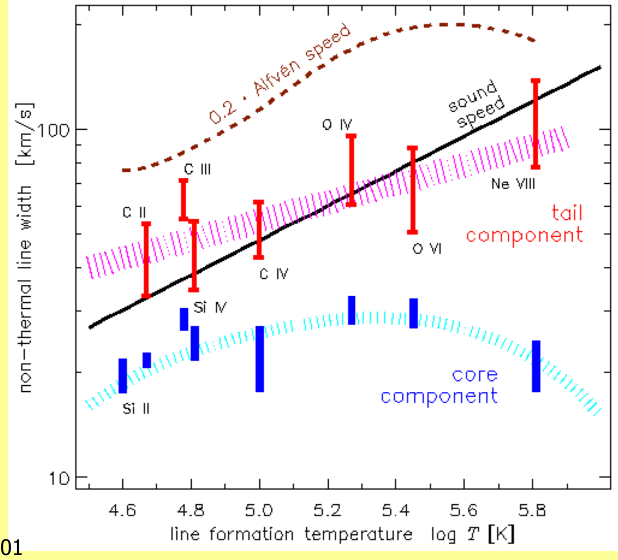

Heavy ion heating by cyclotron resonance

$\Omega \sim Z/A$

Heavy ion temperature

T=(2-6) MK

r = 1.15 R_S

- **Magnetic mirror in coronal funnel/hole**
- **Cyclotron resonance $\Rightarrow$ increase of μ**

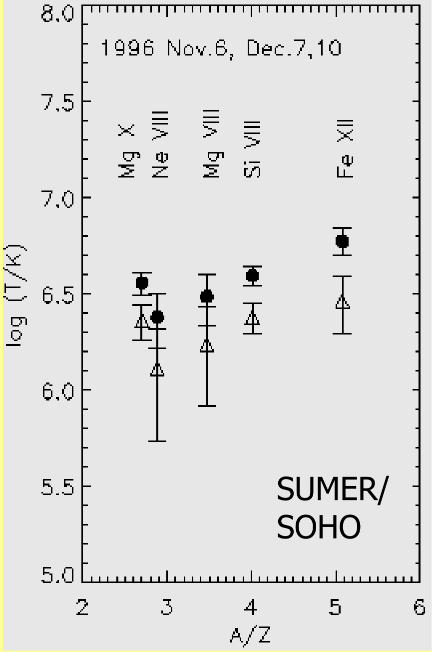

Tu et al., Space Sci. Rev., **87**, 331, 1999

Oxygen and hydrogen thermal speeds in coronal holes

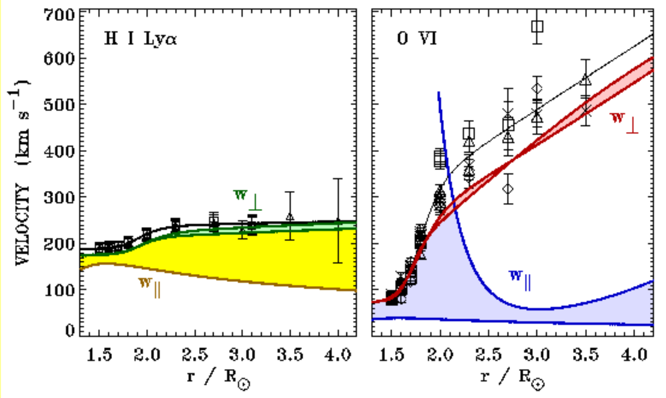

Very Strong perpendicular heating of Oxygen !

Cranmer et al., Ap. J., **511**, 481, 1998

Large anisotropy: $T_{O\perp}/T_{O\|} \geq 10$

Magnetic network with loops

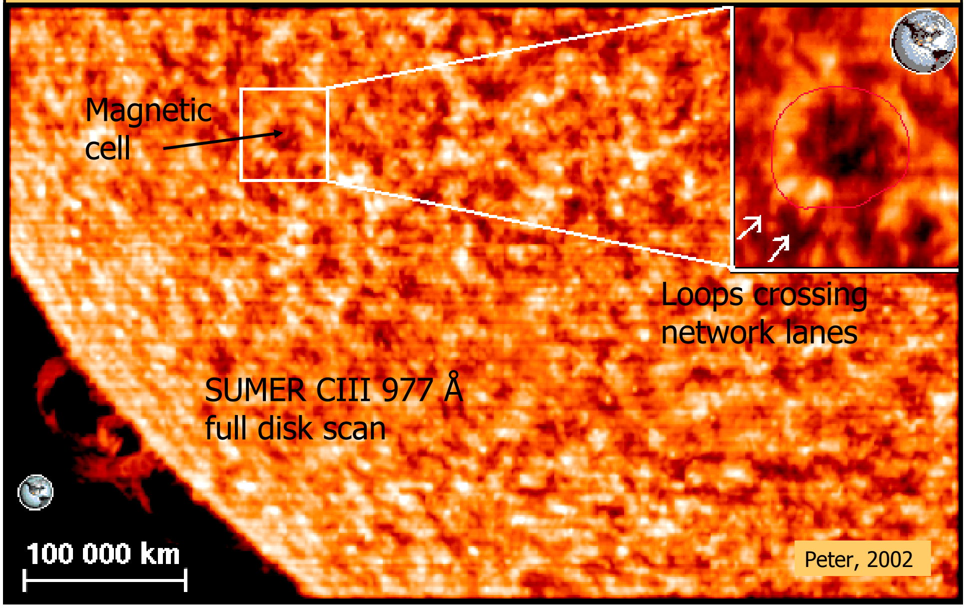

Peter, 2002

The elusive coronal magnetic field

Future: High-resolution imaging and spectroscopy (70 km pixels) of the corona

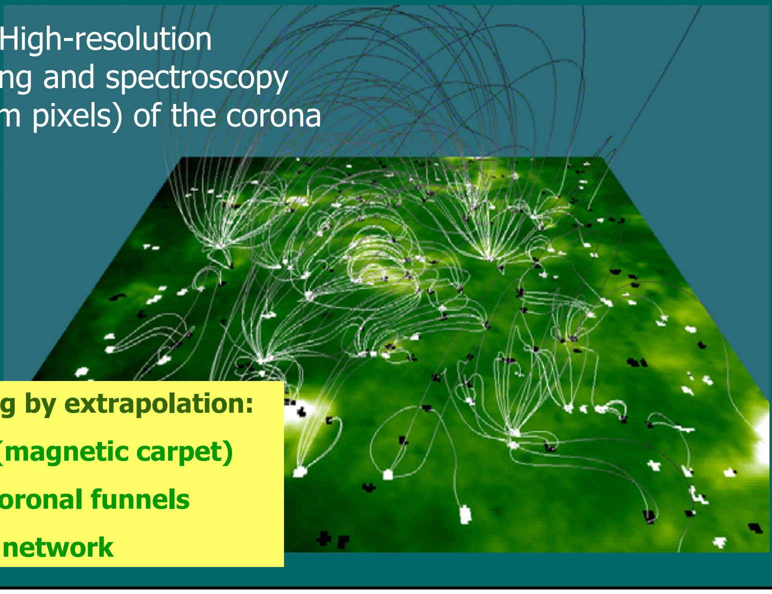

Modelling by extrapolation:

- **Loops (magnetic carpet)**
- **Open coronal funnels**
- **Closed network**

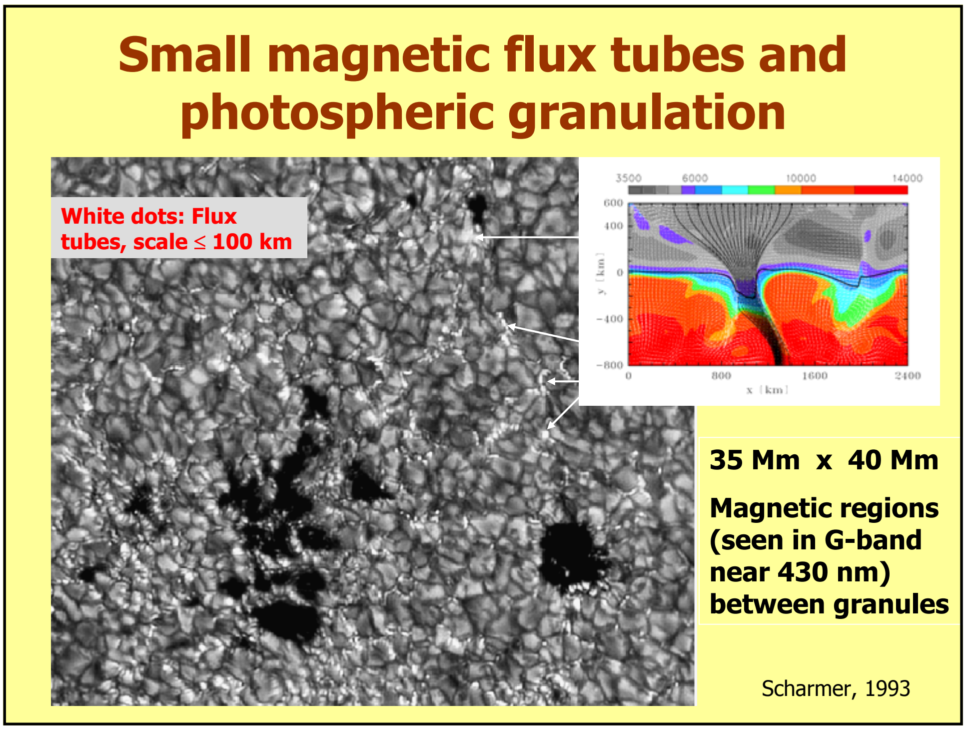

Small magnetic flux tubes and photospheric granulation

White dots: Flux tubes, scale ≤ 100 km

35 Mm x 40 Mm

Magnetic regions (seen in G-band near 430 nm) between granules

Scharmer, 1993

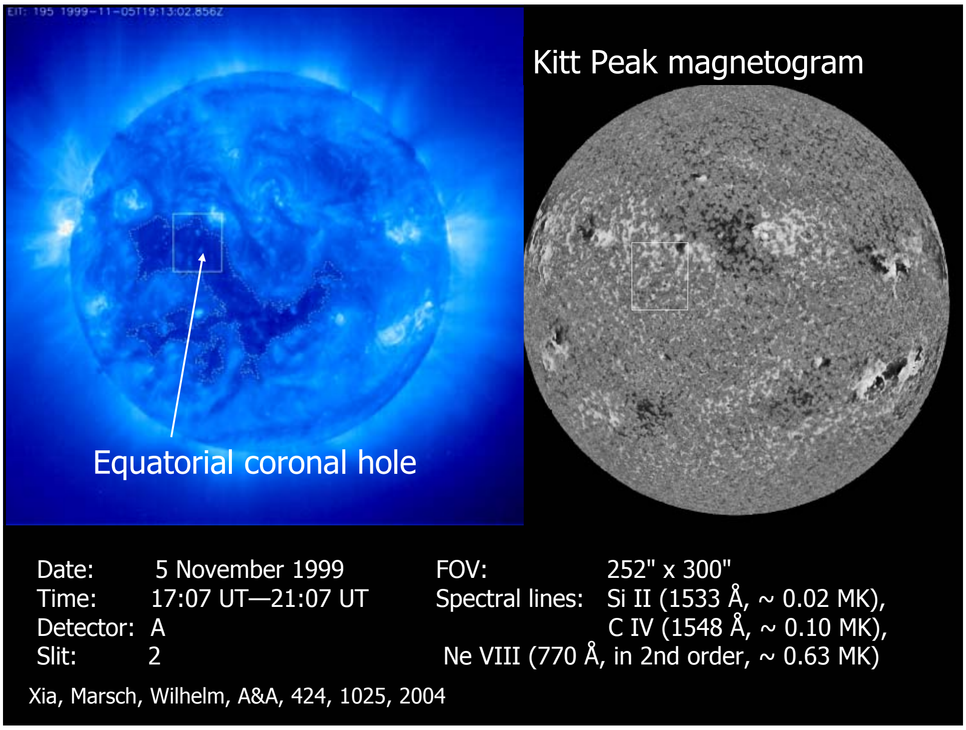

Kitt Peak magnetogram

Equatorial coronal hole

Date: 5 November 1999
Time: 17:07 UT—21:07 UT
Detector: A
Slit: 2

FOV: 252" x 300"
Spectral lines: Si II (1533 Å, ~ 0.02 MK),
C IV (1548 Å, ~ 0.10 MK),
Ne VIII (770 Å, in 2nd order, ~ 0.63 MK)

Xia, Marsch, Wilhelm, A&A, 424, 1025, 2004

Force-free field extrapolation

$$\boxed{j = \alpha B}$$

$$B_x = \sum_{m,n=1}^{\infty} \frac{C_{mn}}{\lambda_{mn}} \exp\left(-r_{mn} z\right) \cdot$$
$$\left[\alpha \frac{\pi n}{L_y} \sin\left(\frac{\pi m x}{L_x}\right) \cos\left(\frac{\pi n y}{L_y}\right) - \right.$$
$$\left. - r_{mn} \frac{\pi m}{L_x} \cos\left(\frac{\pi m x}{L_x}\right) \sin\left(\frac{\pi n y}{L_y}\right)\right] \quad (1)$$

$$B_y = - \sum_{m,n=1}^{\infty} \frac{C_{mn}}{\lambda_{mn}} \exp\left(-r_{mn} z\right) \cdot$$
$$\left[\alpha \frac{\pi m}{L_x} \cos\left(\frac{\pi m x}{L_x}\right) \sin\left(\frac{\pi n y}{L_y}\right) + \right.$$
$$\left. + r_{mn} \frac{\pi n}{L_y} \sin\left(\frac{\pi m x}{L_x}\right) \cos\left(\frac{\pi n y}{L_y}\right)\right] \quad (2)$$

$$B_z = \sum_{m,n=1}^{\infty} C_{mn} \exp\left(-r_{mn} z\right) \cdot \sin\left(\frac{\pi m x}{L_x}\right) \sin\left(\frac{\pi n y}{L_y}\right) \quad (3)$$

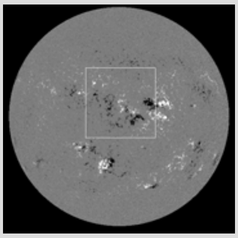

$$r_{mn} = \sqrt{\lambda_{mn} - \alpha^2}.$$

$$\lambda_{mn} = \pi^2 (m^2/L_x^2 + n^2/L_y^2)$$
$$2/L^2 = (1/L_x^2 + 1/L_y^2)$$

definitions

symmetry

$$B_z(-x, y) = -B_z(x, y)$$
$$B_z(x, -y) = -B_z(x, y)$$

Seehafer, Solar Physics **58**, 215, 1978

Magnetic network loops and funnels

Structure of transition region

F_B = AB **F_M = AρV**

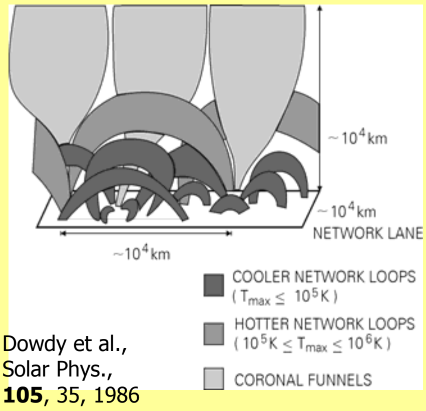

Dowdy et al.,
Solar Phys.,
105, 35, 1986

Magnetic field of coronal funnel

A(z) = flux-tube cross section

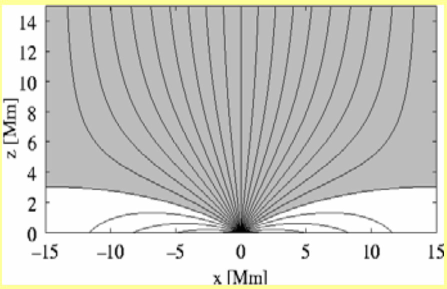

Hackenberg, Marsch and Mann,
Space Sci. Rev., **87**, 207, 1999

Coronal magnetic field extrapolation

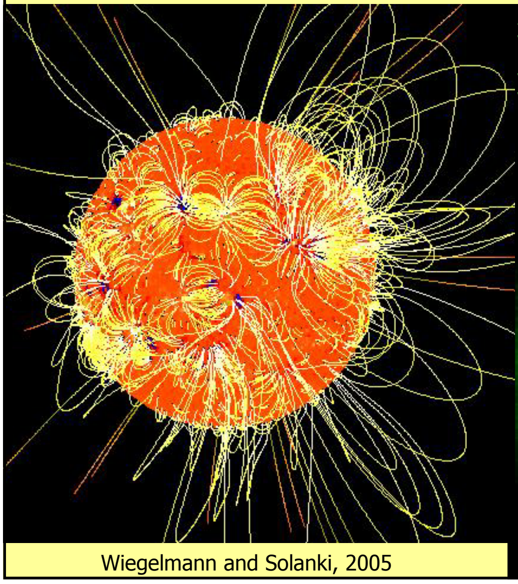

Wiegelmann and Solanki, 2005

Active regions mainly consist of closed magnetic loops, in which plasma is confined and causes bright emission. The large-scale magnetic field is open in coronal holes, from which plasma escapes on open field lines as solar wind, and where the line emission is strongly reduced.

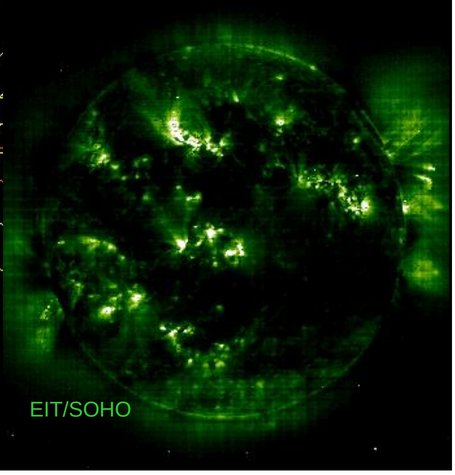

EIT/SOHO

MHD model coronal magnetic field

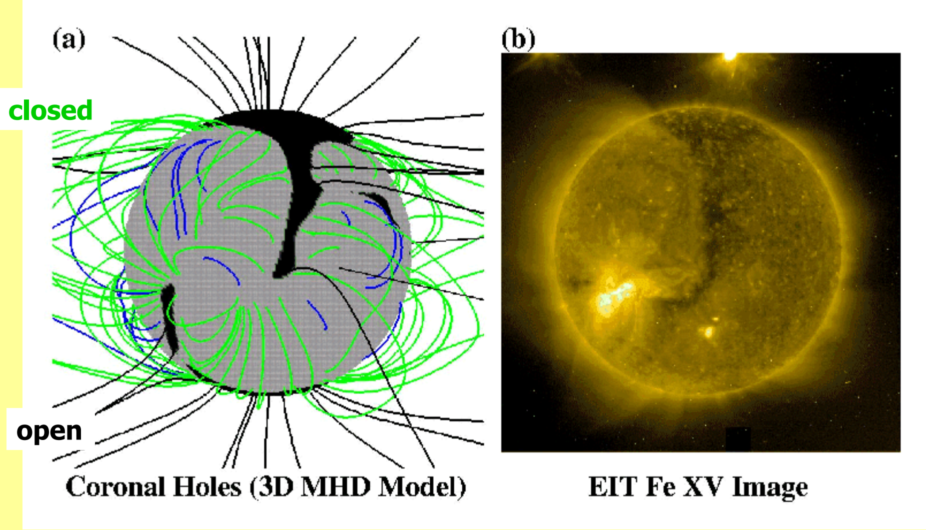

Coronal Holes (3D MHD Model)

EIT Fe XV Image

Linker et al., JGR, **104**, 9809, 1999

„Elephants trunk" coronal hole

The Sun` open magnetic field lines

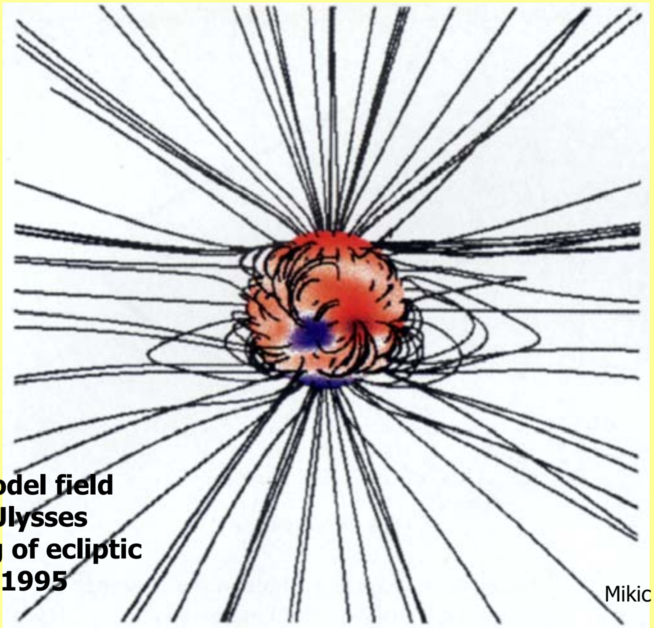

MHD model field during Ulysses crossing of ecliptic in early 1995

Mikic & Linker, 1999

Measuring the polar magnetic field

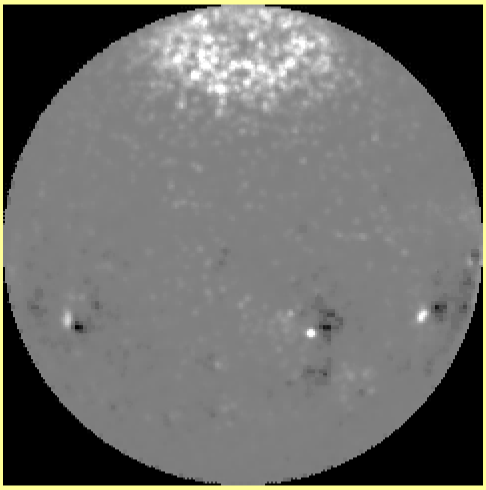

View of the sun from 30° northern latitude

Solar Orbiter will allow us to study the:

- **magnetic structure and evolution of the polar regions,**
- **detailed flow patterns in the polar regions,**
- **development of magnetic structures, using local-area helioseismology at high latitudes.**

Model magnetogram of the simulated solar cycle (courtesy Schrijver).

Summary

- The Sun's corona is highly structured and changes
- The magnetic field consists of loops and funnels
- EUV radiation of the corona is highly structured
- Doppler spectroscopy in EUV enables plasma diagnostics via line shifts, widths and radiances
- The magnetic network is very dynamic
- Small-scale motions and turbulence prevails
- Temperature profiles indicate minor ion heating